High Performance n-Type Field-Effect Transistors Based on Indenofluorenedione and Diindenopyrazinedione Derivatives

Tomohiro Nakagawa,[†] Daisuke Kumaki,[‡] Jun-ichi Nishida,[†] Shizuo Tokito,[‡] and Yoshiro Yamashita*,[†]

Department of Electronic Chemistry, Interdisciplinary Graduate School of Science and Engineering, Tokyo Institute of Technology, Nagatsuta, Midori-ku, Yokohama 226-8502, Japan, and NHK Science and Technical Research Laboratories, Kinuta, Setagata-ku, Tokyo 157-8510, Japan

Received February 5, 2008
Revised Manuscript Received March 7, 2008

Organic field-effect transistors (OFETs) have attracted much attention in recent years owing to advantages such as large-area fabrication and mechanical flexibility leading to their possible applications in electronic devices.[1] Development of new organic semiconductors is very important for the progress in this field. Although some p-type semiconductors such as pentacene show comparable mobilities to amorphous silicon-based FETs,[2] there are a limited number of n-type semiconductors showing higher mobilities than 0.1 $cm^2/(V\ s)$.[3] The development of high-performance n-type semiconductors is strongly required for the fabrication of organic p−n junctions and complementary integrated circuits. To develop novel n-type semiconductors, we have now focused on indenofluorenediones **1** and diindenopyrazinediones **2** for the following reasons. First, the structures of the pentacyclic diones are rigid and planar. Second, they have high electron affinity owing to the presence of the electron-accepting cyclopentadienone moiety. The introduction of a pyrazine unit in **2** is expected to further increase the electron affinity. Third, the preparation is ready and substituents are easily introduced. Although derivative **3** was recently reported to show n-type FET behavior with low mobility,[4] the systematic study on FET properties of **1** and **2** has not been carried out. We report here their preparation, physical properties, crystal structures, and FET characteristics.

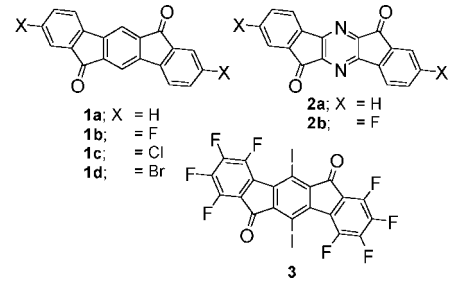

Indeno[1,2-b]fluorene-6,12-dione **1a** was synthesized according to a reported method.[5] The dihalogenated derivatives **1b**−**d** were prepared by a method similar to that described in Scheme 1.[6]

Scheme 1[a]

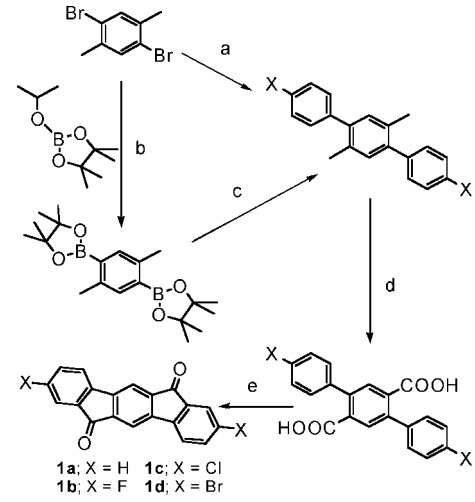

[a] Reagents: (a) $Pd(PPh_3)_4$; phenylboronic acid, 68%; tributyl-(4-fluorophenyl)stannane, 35%; 4-chlorophenylboronic acid, 79%; (b) *t*-BuLi, 47%; (c) $Pd(PPh_3)_4$, 1-bromo-4-iodobenzene, 49%; (d) $KMnO_4$, >99%; (e) conc. H_2SO_4; **1a**, 67%; **1b**, 48%; **1c**, 59%; **1d**, 63%.

Diindeno[1,2-b;1′,2′-e]pyrazine-6,12-dione **2a** was also synthesized according to a reported method.[7] Its fluoro derivative **2b** was obtained as shown in Scheme 2.[8] The compounds **1** and **2** were purified by sublimation several times and characterized by mass spectrometry and elemental analysis.

The electrochemical properties of **1** and **2** were investigated by differential pulse voltammetry (DPV). All the compounds displayed two reduction processes, and no oxidation peaks were observed. The reduction potentials of **1** and **2** are shown in Table 1. These values are relatively high, indicating that they have high electron affinity as expected. Introduction of halogen atoms makes the potentials more positive. The pyrazine analogues **2** have more positive potentials than the corresponding indenones **1**. These facts indicate that the introduction of halogen atoms and the pyrazine rings lower the LUMO levels.

* Corresponding author. E-mail: yoshiro@echem.titech.ac.jp.
[†] Tokyo Institute of Technology.
[‡] NHK Science and Technical Research Laboratories.

(1) (a) Katz, H. E. *Chem. Mater.* **2004**, *16*, 4748. (b) Newman, C. R.; Frisbie, C. D.; da Silva Filho, D. A.; Brédas, J.-L.; Ewbank, P. C.; Mann, K. R. *Chem. Mater.* **2004**, *16*, 4436. (c) Murphy, A. R.; Fréchet, J. M. *J. Chem. Rev.* **2007**, *107*, 1066. (d) Sun, Y.; Liu, Y.; Zhu, D. *J. Mater. Chem.* **2005**, *15*, 53.
(2) (a) Swartz, C. R.; Parkin, S. R.; Bullock, J. E.; Anthony, J. E.; Mayer, A. C.; Malliaras, G. G. *Org. Lett.* **2005**, *7*, 3163. (b) Hajlaoui, M. E.; Garnier, F.; Hassine, L.; Kouki, F.; Bouchriha, H. *Synth. Met.* **2002**, *129*, 215. (c) Roy, V. A. L.; Zhi, Y. G.; Xu, Z. X.; Yu, S. C.; Chan, P. W. H.; Che, C. M. *Adv. Mater.* **2005**, *17*, 1258.
(3) (a) Yoon, M. H.; DiBenedetto, S. A.; Facchetti, A.; Marks, T. J. *J. Am. Chem. Soc.* **2005**, *127*, 1348. (b) Ando, S.; Murakami, R.; Nishida, J.; Tada, H.; Inoue, Y.; Tokito, S.; Yamashita, Y *J. Am. Chem. Soc.* **2005**, *127*, 14996. (c) Jones, B. A.; Ahrens, M. J.; Yoon, M.-H.; Facchetti, A.; Marks, T. J.; Wasielewski, M. R. *Angew. Chem., Int. Ed.* **2004**, *43*, 6363.
(4) Miyata, Y.; Minari, T.; Nemoto, T.; Isoda, S.; Komatsu, K. *Org. Biomol. Chem.* **2007**, *5*, 2592.
(5) Merlet, S.; Birau, M.; Wang, Z. Y. *Org. Lett.* **2002**, *13*, 2157.
(6) Vak, D.; Lim, B.; Lee, S.; Kim, D. *Org. Lett.* **2005**, *19*, 4229.
(7) Ebel, F.; Deuschel, W. *Chem. Ber.* **1956**, *89*, 2799.
(8) York, B. M., Jr. U.S. Patent 4864028, 1989.

10.1021/cm800366b CCC: $40.75
Published on Web 03/20/2008

Scheme 2[a]

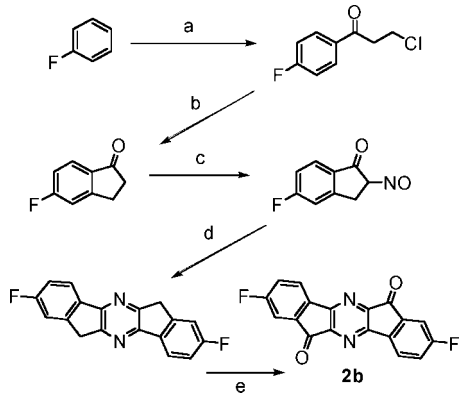

[a] Reagents: (a) $AlCl_3$, 77%; (b) conc. H_2SO_4, 66%; (c) isoamyl nitrite, conc. HCl, 51%; (d) $Na_2S_2O_4$, 44%; (e) $Na_2Cr_2O_7$, 63%.

Table 1. Reduction Potentials and Optical Properties of 1 and 2

compound	E_{red}^1, V[a]	E_{red}^2, V[a]	λ_{abs}, nm[b]	λ_{em}, nm[b]
1a	−1.19	−1.71	297, 335, 484	561, 606
1b	−1.02	−1.52	288, 329	601, 627
1c	−1.05	−1.54	296, 334	578, 613
1d	−1.08	−1.56	296, 335	621
2a	−0.85	−1.44	267, 317, 367, 455	561
2b	−0.75	−1.32	268, 311, 361, 469	591

[a] 0.1 M nBu$_4$NPF$_6$ in DMF, Pt electrode, scan rate 20 mV/s, V vs Fc/Fc$^+$. [b] In DMF.

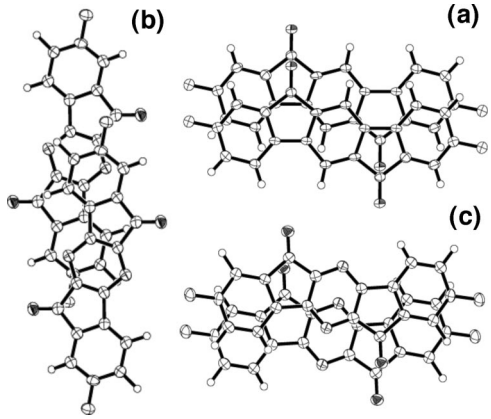

Figure 1. Packing structures of **1b** and **2b** in single crystals. (a) **1b**; (b) red crystal of **2b**; (c) black crystal of **2b**.

Single crystals of **1b** and **2b** were obtained by sublimation, and the crystal structures were determined by X-ray structure analysis. The molecule of **1b** is completely planar and forms a face-to-face π-stacking structure in the crystal as shown in Figure 1a. The columnar structure is formed along the a-axis, where the interplanar distance is 3.30 Å. On the other hand, the pyrazine derivative **2b** shows a polymorphism and afforded two kinds of crystals, red and black ones. These were purified by multiple sublimation. In both crystals, the molecule of **2b** is planar and forms a columnar structure along the a-axis. The interplanar distances between the molecules in the column are 3.22 Å and 3.31 Å in the red and black crystals, respectively. The overlap patterns of molecules are different as shown in Figure 1b,c. In the red crystal only a half of the molecule is overlapped, whereas in the black crystal the whole molecule is involved in the overlap. This difference in the overlap reflects the color of the crystals.

Table 2. Field-Effect Characteristics of 1 and 2 on Bottom Contact Geometry[a]

compound	surface	mobility, cm^2 V^{-1} s^{-1}	on/off ratio	threshold, V
1a	HMDS	no gate effect		
1b	bare	1.9×10^{-4}	6×10^3	+88
	HMDS	0.17	2×10^7	+69
1c	HMDS	1.8×10^{-2}	1×10^7	+56
1d	HMDS	9.9×10^{-3}	4×10^6	+61
2a	HMDS	2.7×10^{-4}	2×10^4	+70
2b	bare	8.8×10^{-4}	2×10^5	+24
(black solid)	HMDS	1.1×10^{-2}	1×10^6	+27
2b	bare	2.7×10^{-4}	2×10^4	+21
(red solid)	HMDS	8.7×10^{-3}	9×10^5	+27

[a] FETs were fabricated on Si/SiO_2. L/W = 25 μm/294 mm, Au electrode. SiO_2 300 nm thick.

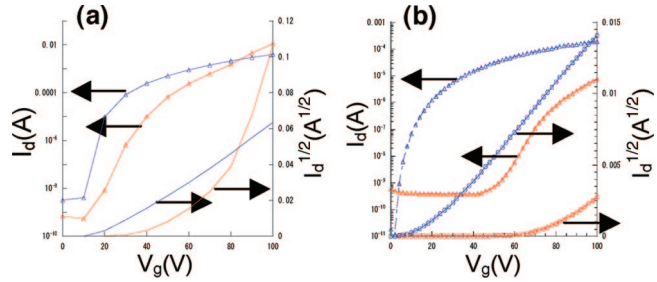

Figure 2. I_d and $I_d^{1/2}$ versus V_g plots for OFET of **1b** (red line) and **2b** (blue line). (a) Bottom-contact device. (b) Top-contact device.

The FET devices based on **1a**−**d** and **2a**,**b** were fabricated on SiO_2/Si substrates by vapor deposition with bottom contact geometry. The SiO_2 gate dielectric was 300 nm and was treated with hexamethyldisilazane (HMDS). The organic semiconductors were deposited at a rate of 0.1−0.3 Å/s. The FET measurements were carried out at room temperature in a high vacuum chamber (10^{-5} Pa). The FET performances are summarized in Table 2. Although the nonsubstituted indenofluorenedione **1a** showed no gate effect, the fluorine substituted derivative **1b** showed n-type FET behavior (Fugure 2a). On the HMDS treated substrate, a high mobility of 0.17 cm^2/(V s) was obtained with a high on/off ratio of 10^7. The mobility is notably high as a bottom contact device and much higher than that of **3** (2.9×10^{-5} cm^2/(V s)).[3] Similarly, the chloro and bromo derivatives **1c**,**d** showed n-type behavior. This result indicates that the two terminal halogen groups induced n-type FET behavior. This is probably attributed to the high electron affinity and/or the better molecular arrangement on the substrate in the halogen-substituted derivatives. When **1b**−**d** were compared, there is a tendency for the mobility to decrease with increasing the halogen atom size, and the threshold voltages were in the range 64 ± 8 V. Diindenopirazinedione derivatives **2a**,**b** also showed n-type FET performances. It should be noted here that the nonsubstituted derivative **2a** showed FET behavior in contrast to **1a**. In the case of **2b**, both red and black crystals of **2b** were used for the device fabrication. However, the difference in the FET performance was not so significant. The threshold voltage of **2b** is greatly reduced compared to that of **1b**. This is due to the decrease of the LUMO levels by the pyrazine rings.

Table 3. Field-Effect Characteristics of 1b and 2b on Top Contact Geometry[a]

compound	surface	mobility, $cm^2\ V^{-1}\ s^{-1}$	on/off ratio	threshold, V
1b	HMDS	6.6×10^{-2}	2×10^4	+75
2b (black solid)	HMDS	0.17	1×10^7	+17

[a] FETs were fabricated on Si/SiO_2. $L/W = 50\ \mu m/1$ mm, Au electrode. SiO_2 200 nm thick.

Higher FET performances are generally observed with top contact geometry than with bottom contact geometry because of better contacts between the electrodes and semiconductors in the former. Therefore, top-contact devices using **1b** and **2b** were fabricated to improve the performances. Gold electrodes were defined after 30 nm of semiconductor deposition by using shadow masks with *W*/*L* of 1.0 mm/50 μm. The SiO_2 gate dielectric was 200 nm thick and treated with HMDS. The performances of these devices are summarized in Table 3, and transfer characteristics are shown in Figure 2b. In the case of **1b**, the top-contact device showed lower performance than the bottom-contact one. This may be attributed to the rough surface of the organic layer leading to the bad contact between the semiconductor layer and the electrodes. On the other hand, the top-contact device of **2b** was increased to 0.17 cm^2/(V s) and the threshold voltage was decreased to 17 V.

The films of these derivatives deposited on SiO_2/Si substrates were investigated by X-ray diffraction in reflection mode (XRD, Figure 3). All compounds showed sharp reflection peaks in the thin films, indicating the high crystallinity and lamella structures. In the thin film of **1b**, the intensity and number of peaks were increased by the HMDS treatment. This fact is consistent with the result of the improved FET performance on the HMDS treated substrate. The *d*-spacing value obtained from the first reflection peak was 13.4 Å, which is close to the molecular length of **1b** (13.7 Å) obtained by X-ray crystal analysis, suggesting that the molecules of **1b** stand on the substrate almost perpendicularly. In the XRD measurement of **2b**, a clear difference depending on the crystal morphology was observed. When the black crystals were deposited on the HMDS treated substrate, two sharp peaks were observed. These peaks were very weak when the red crystals were used. The *d*-spacing value in the thin film of **2b** prepared from the black crystals was 11.2 Å, which is shorter than the molecular length of **2b** (13.5 Å) obtained by X-ray crystal analysis. Thus, the molecules of **2b** are considered to have approximately 35° declining orientation on the substrate.

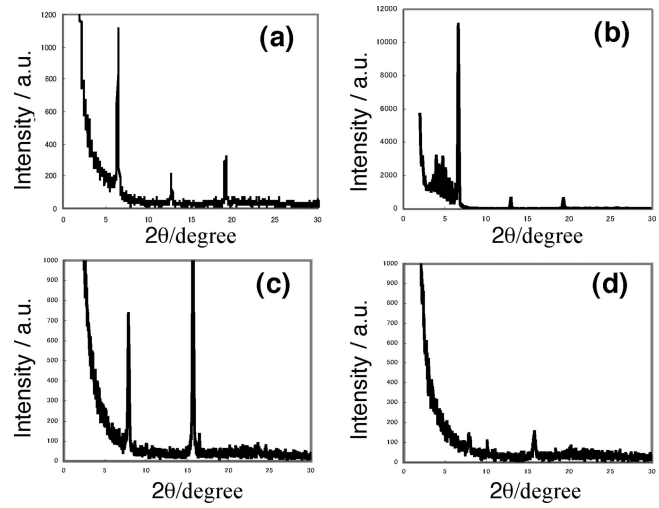

Figure 3. X-ray diffraction of thin films of **1b** and **2b**. (a) Compound **1b** on bare substrate. (b) Compound **1b** on HMDS treated substrate. (c) Compound **2b** (black solid) on HMDS treated substrate. (d) Compound **2b** (red solid) on HMDS treated substrate.

In conclusion, novel indenofluorenedione and diindenopyrazinedione derivatives were developed as n-type semiconductors. Introduction of the halogen groups and/or a pyrazine ring to the indenofluorenedione framework increased the electron affinity, leading to the higher n-type performances. The top-contact device using **2b** showed the highest performance; $\mu = 0.17$ cm^2/(V s) and $V_{th} = 17$ V.

Acknowledgment. This work was supported by a Grant-in-Aid for Scientific Research (No. 15073212, 19350092, 18750165) from the Ministry of Education, Culture, Sports, Science and Technology, Japan, and The Asahi Glass Foundation.

Supporting Information Available: Synthesis, absorption spectra, DPVs, I_d versus V_d and I_d versus V_g characteristics for **1b** and **2b**, and X-ray crystallographic data for **1b** and **2b** (PDF). This material is available free of charge via the Internet at http://pubs.acs.org.

CM800366B